Mathematical Biosciences 338 (2021) 108615

Contents lists available at ScienceDirect

Mathematical Biosciences

journal homepage: www.elsevier.com/locate/mbs

Original Research Article

On how the power supply shapes microbial survival

David Diego [a,b,*], Bjarte Hannisdal [a,b], Håkon Dahle [b,c,d]

[a] Department of Earth Science, University of Bergen, Allégaten, NO-5007 Bergen, Norway
[b] K.G. Jebsen Centre for Deep Sea Research, Allégaten, NO-5007 Bergen, Norway
[c] Department of Biological Sciences, University of Bergen, Thormøhlens gate 53A, NO-5006 Bergen, Norway
[d] Computational Biology Unit, Department of Informatics, University of Bergen, N-5020 Bergen, Norway

ARTICLE INFO

Keywords:
Microbial survival
Power supply
Substrate thermodynamics

ABSTRACT

Understanding how environmental factors affect microbial survival is an important open problem in microbial ecology. Patterns of microbial community structure have been characterized across a wide range of different environmental settings, but the mechanisms generating these patterns remain poorly understood. Here, we use mathematical modelling to investigate fundamental connections between chemical power supply to a system and patterns of microbial survival. We reveal a complex set of interdependences between power supply and distributions of survival probability across microbial habitats, in a case without interspecific resource competition. We also find that different properties determining power supply, such as substrate fluxes and Gibbs energies of reactions, affect microbial survival in fundamentally different ways. Moreover, we show how simple connections between power supply and growth can give rise to complex patterns of microbial survival across physicochemical gradients, such as pH gradients. Our findings show the importance of taking energy fluxes into account in order to reveal fundamental connections between microbial survival and environmental conditions, and to obtain a better understanding of microbial population dynamics in natural environments.

1. Introduction

Microbial communities play key roles in global elemental cycles, medicine, and biotechnology. A fundamental goal of microbial ecology is to understand how various environmental factors and settings influence microbial communities in terms of diversity, stability, and structure. Numerous studies have characterized microbial community patterns across different environmental settings. For example, pH has been found to be a good predictor of microbial diversity in soil [1,2], temperature is correlated with marine planktonic bacterial richness on a global scale [3,4], whereas salinity has been found to be correlated with microbial diversity in lake sediments [5], soils [2,6] and estuaries [7,8]. The supply of organic substrates has been also reported to control the patterns of biodiversity for chemotrophs [9,10].

However, a major challenge in the field of microbial ecology is that our understanding of the underlying dynamics generating such patterns remains very limited [11–15].

Revealing the exact connections between the multiplicity of environmental factors and microbial community structure through analyses of natural environments is, however, extremely challenging due to the high complexity and high number of unknown processes occurring in biological systems. For instance, fluxes of substrate are often difficult to quantify, and extensive co-variation of variables makes it notoriously difficult to pinpoint causal effects.

A complement to exploring natural environments is to use a theoretical modelling approach. Such models do not mimic real systems in detail, but they enable us to represent basic principles in a reproducible way and to formulate testable hypotheses. For example, one may isolate and study the mechanistic relationship between power supply and patterns of microbial survival in a highly idealized community.

Theoretical analyses of models representing the dynamics of highly simplified communities have provided useful insights into the conditions that favour co-existence of species, e.g. in terms of substrate uptake kinetics, [16–19], top down control by grazers [20,21], and metabolic conversion of common substrates [13]. The thermodynamics of chemical reactions of substrates arguably plays an important role in these connections.

Indeed, recent gene-centric analyses of oxygen minimum zones have found that fluxes of energy seem to be robust predictors of microbial productivity and functional community structure [22,23]. Moreover, in hydrothermal systems, the chemical energy landscapes emerging from mixing between reduced hydrothermal fluids and oxygenated cold seawater, seem to shape distributions of functional groups of bacteria and archaea [24,25]. Numerous environmental factors, such as pH, salinity and temperature, affect the Gibbs energies of chemical reactions, and thus modulate the chemical power supply utilized by microbial communities [26,27]. Part of the variation in biodiversity

* Corresponding author at: Department of Earth Science, University of Bergen, Allégaten, NO-5007 Bergen, Norway.
E-mail address: diegocastro.david@gmail.com (D. Diego).

https://doi.org/10.1016/j.mbs.2021.108615
Received 31 December 2020; Received in revised form 29 March 2021; Accepted 4 April 2021
Available online 18 April 2021

observed along physicochemical gradients, such as pH gradients, may therefore ultimately be linked to how those gradients affect energy landscapes. There is a rich literature analysing the emergence of microbial community structure and diversity within a theoretical modelling perspective [28–33]. Interestingly, Marsland et al. [28] show how energy fluxes induce distinct regimes in β-diversity and functional structure of microbial communities analogous to phase transitions in statistical physics.

In our work, we focus our study on the analysis of the connections between the power supply to a system and the resulting patterns of microbial survival, in a case without interspecific resource competition. To that aim, we analyse a highly idealized population dynamics model where growth rates are determined by maintenance powers, uptake rates of substrates, and the Gibbs energy of substrate oxidation. In practical terms, our model describes a one species-one resource system subject to a multiplicity of bio-chemical conditions. We find a highly complex set of interdependences between power supply and patterns of microbial survival, as we shall see. Based on our findings, we also propose hypotheses about the connection between power supply and simple microbial communities that could be tested in the laboratory and evaluated in studies of natural environments.

2. The model

In our model, we will describe a habitat, or a subset of a habitat, occupied by a single species feeding on a single substrate. The substrate enters the habitat (or system) at a fixed rate (Fig. 1). We will consider multiple bio-chemical and environmental conditions, including the substrate itself, in this hypothetical habitat. Within our model, each particular instance of the habitat environmental conditions, including the organisms populating the habitat, will be called a *niche*.

It is worth noting that simple communities, where there is no competition for limiting substrates between functional groups can be reconstructed, using microbial strains from culture collections, as artificial communities in laboratory settings. Hence, our modelling results are in principle testable. It should also be noted that there is growing evidence that environmental energetic constraints largely determine the community structure of metabolic functional groups (but not necessarily taxonomic groups) in both industrial bioreactors and in environmental samples [22,34–38]. Based on our model, we can analyse how the community structure of metabolic functional groups is shaped by power supply alone without any influence from more or less complex interactions between the functional groups.

In our model, niches and substrates will be labelled as $\{1, \dots, N\}$ such that the substance S_i acts as the substrate for the ith niche. At any given instant of time t, $c_i(t)$ will denote the number of cells per unit volume occupying the habitat when the conditions corresponding to the ith niche are considered. $c_i(t)$ will be called the *cellular abundance* or simply *abundance* in the ith niche. We take c_i to have units of cell cm^{-3}. Similarly, $s_i(t)$ will denote the amount of substrate of type i (measured in mol) per unit volume, so that $s_i(t)$ has units of mol cm^{-3}. Limiting substrates enter the system at a fixed rate λ (s^{-1}). Cellular substrate uptake rates depend on substrate concentrations in the system, and are modelled according to Michaelis–Menten kinetics as:

$$\rho_i(s_i) = r^i_{max}\,\frac{s_i}{k + s_i}\,, \tag{1}$$

where r^i_{max} (mol s^{-1}) denotes the maximum uptake rate and k (mol cm^{-3}) is the half-saturation concentration,[1] that is: $\rho_i(k) = r^i_{max}/2$. We remark that we allow different values of the maximum uptake rate across different niches, hence the super index i in r^i_{max}. The value r_{max} in Fig. 1 serves here as an order of magnitude for the typical value of the uptake rate. Once absorbed by a cell, the ith substrate (S_i) undergoes a chemical reaction of the type $S_i + a_1A_1 + \cdots + a_nA_n \longrightarrow b_1B_1 + \cdots + b_mB_m$, with $A_1, \dots, A_n$ denoting any other reactants than S_i and $B_1, \dots, B_m$ denoting products. The Gibbs energy of the chemical reaction for each mole of the substrate of type i, ΔG^i_r, in turn depends on the reactants/products concentrations as

$$\begin{aligned}\Delta G^i_r &= \Delta G^{0i}_r + RT\ln\frac{\prod_j[B_j]^{b_j}}{[S_i]\prod_k[A_k]^{a_k}}\,,\\ &= \Delta G^{0i}_r + RT\ln\frac{\prod_j[B_j]^{b_j}}{\prod_k[A_k]^{a_k}} - RT\ln[S_i]\,,\end{aligned} \tag{2}$$

where ΔG^{0i}_r denotes the standard free Gibbs energy for the reaction, R is the ideal gas constant and T is the temperature. Moreover, $[\cdot]$ denotes the molar concentration, and hence $s_i = [S_i]$. For simplicity, we assume the activity coefficients for all reactants and products to be 1. We also consider a situation where $s_i \ll [A_j]$ and $s_i \ll [B_k]$, that is: only the substance S_i is limiting, and we assume that the consumption or production of substances A_j and B_k due to the growth of the organisms in the ith niche, does not affect in any significant way the molar concentrations of these substances in the system. An example of the class of reactions modelled in our work could be found in an aerated environment (with constant and high O_2 concentration) where various organic or inorganic electron donors (such as NO_2^-, H_2, H_2S, CH_4, formate, acetate, glucose) enter the system at fixed rates and are oxidized into products (CO_2/HCO_3^-, SO_4^{2-}, NO_3^-) by microbial species (or functional groups) that grow on one limiting electron donor each. For example, the glucose oxidizers would obtain energy from the reaction 1 $C_6H_12O_6$ + 6 O_2 → 6 CO_2 + 6 H_2O. For this reaction, glucose would be denoted as S in our model, O_2 would be denoted as A_1, and CO_2 and H_2O would be denoted as B_1 and B_2, respectively. Similarly, one could imagine an anaerobic environment of microbial species (or functional groups) using a set of redox pairs with unique electron donors (e.g. CH_4/ SO_4^{2-}, acetate/SO_4^{2-}, H_2/ NO_3^-) and where each electron donor is the limiting substrate for the respective species or functional group. However, it should be emphasized that our model assumes that there is no interspecific competition for resources. This assumption may be valid for certain simple artificial communities grown in the laboratory, but it is a simplification regarding most or all natural environments.

In order to keep the number of symbols used in this work as low as possible, we will make a slight abuse of notation and refer to the combination $\Delta G^{i0}_r + RT\ln\frac{\prod_j[B_j]^{b_j}}{\prod_k[A_k]^{a_k}}$ simply as the standard Gibbs energy of the reaction involving the ith substrate, and we will re-denote such quantity again as ΔG^{0i}_r. We stress that at no point in this work we will consider variations neither in the temperature nor in the pressure.

In our work, we thus take into account that the energy available from the ith reaction (measured in J mol^{-1}), which is used as an energy source in the ith niche, depends on the substrate concentration as

$$E_i(s_i) = -\Delta G^i_r = -\Delta G^{0i}_r + RT\ln s_i\,. \tag{3}$$

In a recent work, [39], the authors study a population dynamics model for chemotrophs in anaerobic conditions where the dependence of the energy available from a redox reaction on the concentration of the reaction constituents, is also considered. More specifically, the authors study a single microbe feeding on a redox reaction of the type $A_d + B_a \to A_a + B_d$ where the total concentration $A_a + A_d$ is constant and the individual concentrations B_a and B_d are also constant. The variation of A_d is, in their model, uniquely determined by the consumption rate and the abiotic reaction rates. In addition, the authors focus their study in the analysis of the dependence of the steady state population density on the ability of the microbe to absorb the substrate. In our case, we consider a chemostat scenario and we focus our attention on how the power supply to the system shapes the patterns of microbial survival.

[1] In order to reduce the multiplicity of constants, we take a common value for the half-saturation constant.

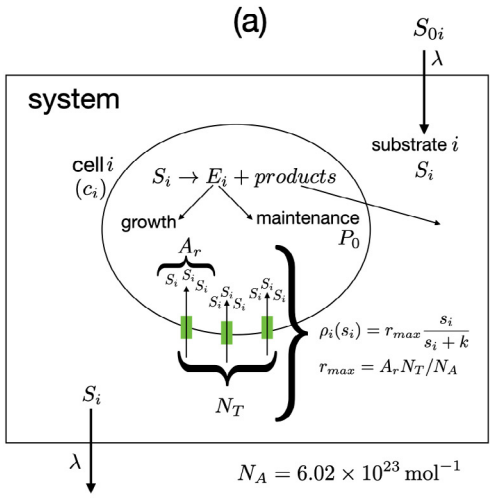

(b)

Symbol	Parameter	Magnitude	Units
P_0	maintenance power	10^{-13}	$\frac{\mathrm{J}}{\mathrm{s\cdot cell}}$
N_T	♯ transporters	10^4	-
A_r	max. absorp. rate	10^4	$\frac{\mathrm{molecule}}{\mathrm{s\cdot transporter}}$
k	saturation const.	10^{-6}	$\mathrm{mol/cm^3}$
λ	flowrate	10^{-8}	$\mathrm{s^{-1}}$
r_{max}	max. uptake rate	10^{-16}	mol/s
T	Temperature	300	K

Fig. 1. (a) Model Schematic: Substrates flow into and out of a system with a fixed flowrate (λ). The power supply of the ith substrate is defined as the product substrate specific inflow concentration (S_{0i}), the flowrate (λ) and the energy available from each mole of substrate (E_i). Once the ith substrate enters the system it is homogeneously distributed in the system to the concentration s_i. The ith substrate is consumed at a rate (ρ_i) dependent on s_i, modelled according to Michaelis–Menten kinetics in Eq. (1), so that the uptake of the ith substrate in the ith niche is the product between ρ_i and the population concentration within the ith niche (c_i). The cell specific power supply is the product $E_i\rho_i$. Cellular growth rates depend on the power available for growth after a fixed amount of power has been used for maintenance Eq. (4a). The maximum uptake rate is a derived constant obtained as $r_{max} = N_T A_r / N_A$, with N_A denoting the Avogadro number. (b) Values and units of model constants. See the Supplementary Information (SI) for details.

We assume in our model that all organisms have a maintenance power demand, P_{0i} with units J $\mathrm{s^{-1}}$ $\mathrm{cell^{-1}}$. As in several previous studies [40–42], maintenance power is defined here as the power necessary to perform all cellular processes except for growth. This includes power used in spilling reactions [43–45] and power spent on 'useful' functions (e.g. motility). How fast the population in the ith niche grows depends on the power available for new biomass production. This power is the difference between the substrate-consumption power $E_i(s_i)\rho_i(s_i)$, and maintenance power P_{0i}. The rate of change in substrate concentrations in the system is defined by the flow of substrate in and out of the system, as well as the rate of consumption of the substrate. All the above considerations lead to the following set of ODEs:

$$\dot{c}_i = Y_i \left[E_i(s_i)\rho_i(s_i) - P_{0i}\right] c_i\,, \tag{4a}$$

$$\dot{s}_i = \lambda(S_{0i} - s_i) - \rho_i(s_i)c_i\,, \tag{4b}$$

where we remark again that each index $i \in \{1, \dots, N\}$ labels a particular niche, i.e., a particular set of bio-chemical and environmental conditions in the modelled habitat. In addition, Y_i (cell $\mathrm{J^{-1}}$) is the biomass yield, i.e. the number of cells that can be built from each unit of energy, λ ($\mathrm{s^{-1}}$) is the flowrate entering the system and S_{0i} (mol $\mathrm{cm^{-3}}$) is the input concentration for the ith substrate. In Fig. 1b we provide typical values for several of the model constants. Unless otherwise specified, these values are used in the numerical experiments.

2.1. Stationary solutions

In the Supplementary Information (SI) we show the main properties of the dynamics generated by the set of differential equations given in Eq. (4). The stationary solutions correspond to

$$Y_i \left[E_i(s_i^*)\rho_i(s_i^*) - P_{0i}\right] c_i^* = 0\,, \tag{5a}$$

$$\lambda(S_{0i} - s_i^*) - \rho_i(s_i^*)c_i^* = 0\,, \tag{5b}$$

for all $1 \le i \le N$. The non trivial stationary solution ($c_i^* > 0$) requires

$$E_i(s_i^*)\rho_i(s_i^*) = P_{0i}\,. \tag{6}$$

This is a transcendental equation but one may find a closed expression for its solution in terms of the Lambert W-function[2] as (see SI for details)

$$s_i^* = \frac{\frac{kP_{0i}}{r^i_{max}RT}}{W\left(\frac{kP_{0i}}{r^i_{max}RT}\, e^{-\frac{r^i_{max}\Delta G_r^{0i} + P_{0i}}{r^i_{max}RT}}\right)}\,. \tag{7}$$

The corresponding asymptotic value for the cellular abundance in the ith niche is then

$$c_i^* = \lambda\frac{S_{0i} - s_i^*}{\rho_i(s_i^*)} = \frac{\lambda}{P_{0i}}\, E^i_{eq}\left[S_{0i} - e^{\frac{E^i_{eq} + \Delta G_r^{0i}}{RT}}\right]\,, \tag{8}$$

where

$$E^i_{eq} \equiv E_i(s_i^*) = -\Delta G_r^{0i} + RT\ln s_i^*\,, \tag{9}$$

is the asymptotic value for the energy available from the ith substrate. In order to extract some intuition as to how big is the departure of the available energy, E^i_{eq}, from the reaction standard Gibbs energy, ΔG_r^{0i}, we consider a generic niche with model parameter values set as in Fig. 1b, more precisely:

$$-\frac{E_{eq}}{\Delta G_r^0} = 1 - RT\frac{\ln s^*}{\Delta G_r^0}\,, \qquad s^* = \frac{\frac{kP_0}{r_{max}RT}}{W\left(\frac{kP_0}{r_{max}RT}\, e^{-\frac{r_{max}\Delta G_r^0 + P_0}{r_{max}RT}}\right)}\,.$$

We note the existence of a drop in the available energy with respect to ΔG_r^0 (Fig. 2). This is a consequence of the highly non-linear dependence of s^* on ΔG_r^0 through the Lambert W-function.

It can be shown that if $s_i^* < S_{0i}$, for every $1 \le i \le N$, every solution to the above system with $c_i(0) > 0$ and $s_i(0) > 0$, for all $1 \le i \le N$, verifies that $\lim_{t\to\infty} c_i(t) = c_i^*$ and $\lim_{t\to\infty} s_i(t) = s_i^*$, for all $1 \le i \le N$ (for the formal proofs, see SI).

2.2. Patterns of microbial survival

If the steady state value for cellular abundance in the ith niche is non vanishing, $c_i^* > 0$, the corresponding niche will be called *viable*. In addition, given a fixed number of modelled niches N, and assuming equal probabilities for the different habitat environmental conditions, one may estimate the probability for surviving in the conditions

[2] The Lambert W-function, $W(z)$, is implicitly defined as $W(z)e^{W(z)} = z$.

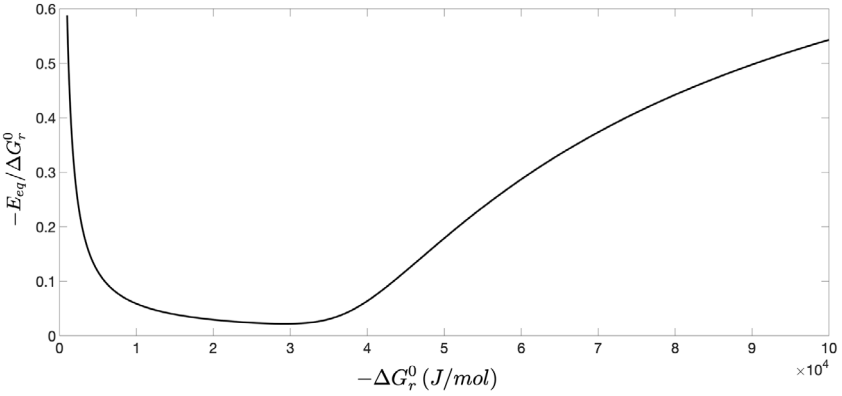

Fig. 2. Ratio between the available energy, E_{eq}, and the reaction standard Gibbs energy, ΔG_r^0, as a function of ΔG_r^0. The model parameters are set as in Fig. 1b.

defining the ith niche as (see SI)

$$b_i := \frac{c_i^*}{\sum_{j=1}^N c_j^*}\,. \tag{10}$$

In order to quantify how the different environmental conditions affect the number of viable niches as well as how diverse is the survival probability, b_i among these, we will employ methods pertaining to quantitative biological diversity. Although there is no unequivocal or precise definition of the concept of biological diversity [46], strong efforts have been committed into finding a unified quantification for it over the last 50 years. In his seminal work in 1973, Hill [47] unified three of the most popular quantifications of biodiversity (Shannon index, Simpson index and the count of the total number of species present) under a common measure which is closely related to the generalized Rényi entropies, and which has become commonly known as Hill numbers. Hill numbers were further extended to account for other aspects of diversity such as phylogenetic diversity (for a review see [48]). Despite all the efforts and theoretical advances over the last decades, the quest for a unified measure of biodiversity is still a challenge [49]. In this work, we will use the Shannon index as the measure for the "diversity" of microbial survival and it will be computed as

$$H_B = -\sum_{i=1}^N b_i \ln b_i\,, \tag{11a}$$

$$b_i = \frac{c_i^*}{\sum_{j=1}^N c_j^*}\,. \tag{11b}$$

In the context of our model, the quantity H_B will be called the *survival diversity*. In essence, this quantity provides information not only on the number of viable niches (those for which $b_i > 0$) but also on the distribution of the values b_i across niches, i.e., how diverse are the survival probabilities across niches. To understand this, suppose that among all viable niches, the survival probability is roughly the same, i.e. $b_i \sim 1/N_v$, where N_v denotes the number of viable niches. From its definition (Eq. (11)) it easily follows that $H_B \sim \ln N_v$. For a generic distribution of values b_i over N_v viable niches, one has that $0 \le H_B \le \ln N_v$ and H_B vanishes only if for some index, i, $b_i = 1$ (and hence the rest vanish), in other words: there is only one viable niche (the previous inequalities are well-known properties of the Shannon functional). We remark the functional dependence of H_B on the "relative abundances" $\frac{c_i^*}{\sum_j c_j^*}$ coincides exactly with the Shannon index for computing the biodiversity of species.

2.3. Diversity of power supply

The instantaneous power supply to the ith niche is defined as

$$P_s^i(t) = \lambda S_{0i}\left[-\Delta G_r^{0i} + RT\ln s_i(t)\right]\,, \tag{12}$$

so that

$$\lim_{t\to\infty} P_s^i(t) = \lambda E_{eq}^i S_{0i} =: P_s^i\,. \tag{13}$$

Our main interest in this work is to compare the survival diversity (as defined above) with the dispersion in the values of the power supply to each niche. Hence, in order to not introduce any artefact in the comparison, we will compute the dispersion in the values of the power supply using the same functional (Shannon index) and the corresponding value will be called, in analogy, diversity of power supply. It will be computed as

$$H_P = -\sum_{i=1}^N p_i \ln p_i\,, \tag{14a}$$

$$p_i = \frac{P_s^i}{\sum_{j=1}^N P_s^j}\,. \tag{14b}$$

3. Relationships between survival diversity and diversity of power supply

At population equilibrium, for any given niche i, its power supply (P_s^i, Eq. (13)) is determined by the flowrate (λ), the input substrate concentration (S_{0i}) and the reaction energy (E_{eq}^i, Eq. (9)) whereas, in terms of the power supply, the abundance of cells for the ith niche (c_i^*, Eq. (8)) is expressed as

$$c_i^* = \frac{P_s^i}{P_{0i}}\left[1 - \frac{1}{S_{0i}} e^{\frac{E_{eq}^i + \Delta G_r^{0i}}{RT}}\right]\,. \tag{15}$$

so even in a simplistic model such as ours, the power supply does not determine uniquely the niche abundance. In addition, the survival probability distribution across niches ($b_i = \frac{c_i^*}{\sum_j c_j^*}$) can be expressed in terms of the "relative abundance" of power supply ($p_i = \frac{P_s^i}{\sum_j P_s^j}$) as

$$b_i = p_i\beta_i\,, \qquad \text{with} \qquad \beta_i = \frac{\frac{1}{P_{0i}}\left[1 - \frac{1}{S_{0i}} e^{\frac{E_{eq}^i + \Delta G_r^{0i}}{RT}}\right]\sum_j P_s^j}{\sum_j \frac{P_s^j}{P_{0j}}\left[1 - \frac{1}{S_{0j}} e^{\frac{E_{eq}^j + \Delta G_r^{0j}}{RT}}\right]}\,. \tag{16}$$

From this, the quantity H_B is expressed as

$$H_B = -\sum_i b_i \ln b_i = -\sum_i p_i\beta_i \ln\left(p_i\beta_i\right)\,, \tag{17}$$

and hence it has no simple functional relationship with $H_P = -\sum_i p_i \ln p_i$. In the following, we investigate the relation between these quantities. As we shall see, in general the diversity of power supply turns out to be a good predictor for the survival diversity. We remark that, within our model, the relevant parameters are those listed in Table 1.

Table 1
Relevant parameters in our model.

Relevant parameters	Symbol
Input substrate concentrations	S_{0i}
Reaction standard Gibbs energies	ΔG_r^{0i}
Uptake rates	r^i_{max}
Maintenance powers	P_{0i}

3.1. How well does H_P determine H_B?

In order to assess how good a determinant of the survival diversity (H_B, Eq. (11)) is the diversity of power supply (H_P, Eq. (14)), we will study how the relevant parameters (Table 1) shape the relationships between both. As we will see, these parameters have significantly distinct effects on the relation between H_P and H_B. As a reference, when all niches share the same values for these parameters (so that in essence there is only one niche available), it turns out that H_B and H_P are virtually in 1-to-1 correspondence and in fact $H_B = H_P$ (Fig. 3).

We start by considering how the relationship between the survival diversity (H_B) and the diversity of power supply (H_P) is shaped by the input substrate concentration (S_{0i}). To this aim, we fix the remaining parameters as common to all niches and given the values in Fig. 1b, that is: $P_{0i} = P_0$ and $r^i_{max} = r_{max}$. Furthermore, we consider a situation where the chemical reactions involving the substances consumed by the organisms, all have roughly the same standard Gibbs energy, that is: no variability in ΔG_r^{0i} across niches. More precisely, $\Delta G_r^{0i} = \Delta G^0_r$, where $-\Delta G^0_r$ will be allowed to take values in the range $10^3 - 10^5$ J mol^{-1}. As for the variability in the input concentration of substrates, we will assume S_{0i} to follow a distribution of the form $S_{0i} \sim S_0\, e^{-\frac{(i-N/2)^2}{\sigma^2 N^2}}$, where N denotes the number of modelled niches, which will vary on the range 10–1000, and σ controls the width of the distribution. This intends to model a situation where only a certain fraction of niches have abundance of substrates, modulated by σ. Small values of σ ($\sigma \sim 0.01$) correspond to a situation in which a very small fraction of the available niches have abundance of substrates. Larger values of σ ($\sigma \gtrsim 10$), however, describe a situation where roughly all available niches have the same abundance of substrates. The reason behind the choice of a Gaussian profile is simply to have a unimodal distribution (i.e., having a single peak). As for the symmetry of the distribution, we remark that its shape has no biological bearing, because the labelling we have adopted is completely arbitrary. The results would be the same using different unimodal distributions such as Log-Normal. Here, we consider a symmetric distribution for simplicity reasons exclusively.

When only a very small fraction of niches have abundance of substrates, the power supply diversity (H_P) fails to determine uniquely the survival diversity (H_B) (Fig. 4a) with a significant dispersion of values for H_B, given a value for H_P. Such a dispersion progressively reduces as the fraction of niches with access to an abundance of substrates increases (Fig. 4b) and when larger fractions of the niches have abundance of input substrates, the power supply becomes a very good predictor of the survival diversity (Fig. 4c and d). The relationship between both being linear, i.e. $H_B \simeq H_P$.

A non-uniform distribution of reaction energies across substrates seems to have a mild effect on the relation between H_B and H_P. To illustrate this, we now fix a common input concentration for all substrates while we consider a distribution of reaction standard Gibbs energies of the form $\Delta G_r^{0i} \sim \Delta G^0_r\, e^{-\frac{(i-N/2)^2}{\sigma^2 N^2}}$ where, as before, $-\Delta G^0_r \in [10^3, 10^5]$ J mol^{-1}. The remaining parameters are set as common to all niches. In this case, the power supply is a robust predictor of the survival diversity and indeed $H_B \simeq H_P$ (Fig. 5).

A yield-cost trade-off is an important trade-off in energy management of living organisms [50–52]. In our model, we incorporate such a trade-off by assuming that high uptake rates (which favour a higher yield) come with an energetic cost in the form of higher maintenance power, which induces a lower yield. In particular, we will consider distributions of uptake rates (r^i_{max}) and maintenance powers (P_{0i}) across niches of the form $r^i_{max} \sim r_{max} e^{-\frac{(i-N/2)^2}{\sigma^2 N^2}}$ and $P_{0i} \sim P_m e^{-\frac{(i-N/2)^2}{\sigma^2 N^2}}$, respectively, while keeping the remaining model parameters as common to all niches. We remark that the trade-off does not refer to the particular values of r^i_{max} and P_{0i}, but to the opposite effects that these values have on the organisms, that is: a higher uptake rate, r^i_{max}, is beneficial while a higher value of P_{0i} is a disadvantage (higher energy demands). Making a mild abuse of language, this situation will be referred to as a trade-off between uptake rate and maintenance power. The effect of such a trade-off in the relation between the diversity of power supply and the survival diversity is also rather mild so that it does not deviate substantially from the linearity (Fig. 6).

For completeness, we consider how non-uniform distributions of all the above relevant model parameters affect the relationship between H_B and H_P, when considered simultaneously. Again one observes that for narrow distributions of the parameters across the niches, the power supply does not determine the survival diversity uniquely (Fig. 7a and b) but more interestingly, the relationship between H_B and H_P departs clearly from the overall linearity shown in the previous cases, maybe with the exception of Fig. 4a.

3.2. How the model parameters affect the survival probability

In the previous section we have considered how the relationship between the diversity of power supply and the survival diversity is modified or affected by the relevant parameters of our model (Table 1). In this section, we turn our attention to the specific effect of these parameters on the survival probability distribution over the niches, $b_i = \frac{c_i^*}{\sum_j c_j^*}$ in Eq. (10). As we shall see, the different model parameters shape survival patterns in substantially different ways.

Non-uniform distributions of input substrate concentrations (S_{0i}) have a mild effect on b_i, at least regarding its dependence on the standard Gibbs energy of reactions ΔG^0_r (Fig. 8). Notice how, as expected, as the distribution of S_{0i} flattens, b_i approaches the uniform distribution, that is: $b_i \sim \frac{1}{N}$, N denoting the number of modelled niches (Fig. 8c and d). The variability in reaction Gibbs energies across niches, in contrast, has a significant impact on the survival probability distribution. Interestingly, there seems to be a bottle neck effect for $-\Delta G^0_r \sim 2 \times 10^4$ J mol^{-1}, where the survival probability is roughly the same for all niches (Fig. 9). A trade-off between uptake rates and maintenance powers turns around the relative viability between niches with respect to the previous cases, such that the most viable niche (that with the highest b_i value) is the one with lowest values for both uptake rate and maintenance power ($i = 1$ and $i = 50$), while the least viable (lowest b_i value) is the one with highest values of both parameters (Fig. 10). Interestingly enough, the combination of non-uniform distributions of values of the above parameters arguably has a more complex impact on the survival probability than when individually considered (Fig. 11). Remarkably, the particular identity of the most viable niche is in this case energy-scale dependent and there seems to be a sharp transition at $-\Delta G^0_r \simeq 3 \times 10^4$ J mol^{-1} (Fig. 12). For relatively peaked distributions of the values of the parameters across niches, the most viable niche for low values of the reaction Gibbs energies ($-\Delta G^0_r \lesssim 2 \times 10^4$ J mol^{-1}) becomes virtually one of the least viable for higher energy scales ($-\Delta G^0_r \gtrsim 8 \times 10^4$ J mol^{-1}) (Fig. 11a and b). The values for the available energy, E^i_{eq}, are roughly the same for all niches and comparatively small on the range $-\Delta G^0_r \sim 2 - 4 \times 10^4$ J mol^{-1} (Fig. 13). In contrast, the energy availability is more markedly different across niches for $-\Delta G^0_r \gtrsim 4 \times 10^4$ J mol^{-1}, the niches with the highest uptake rate ($i = 25$) being the most energetically advantaged (Fig. 13a and b). For $-\Delta G^0_r \lesssim 2 \times 10^4$ J mol^{-1} however, the $i = 25$ niche is one of the least energetically advantaged. The energetic disadvantage of the $i = 25$ niche for $-\Delta G^0_r \lesssim 2 \times 10^4$ J mol^{-1} is clearly reflected in its low viability over these energy scales (Fig. 11). Interestingly, for $-\Delta G^0_r \gtrsim 5 \times 10^4$ J mol^{-1}, the $i = 25$ niche is not the most viable

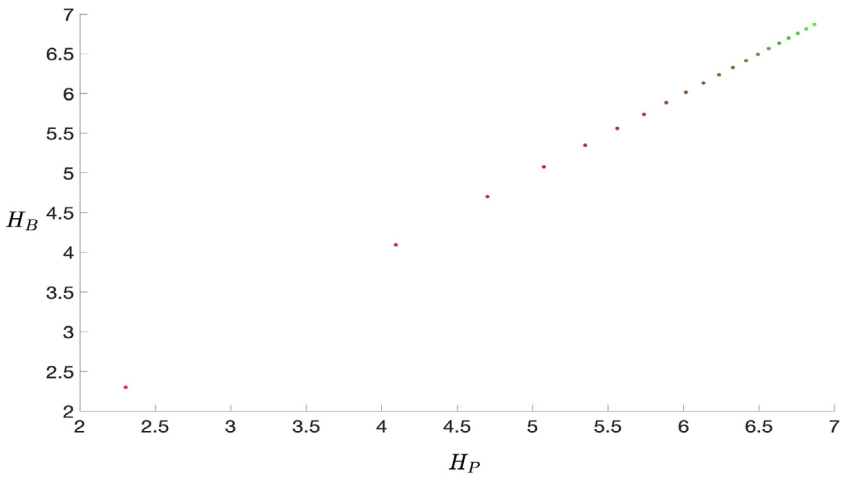

Fig. 3. Survival diversity (H_B) vs. diversity of power supply (H_P) when the model parameters are common to all niches and given the values in Fig. 1b. The graphic shows all pairs (H_P, H_B) corresponding to the considered instances of number of modelled niches, $N \in [10, 1000]$ in steps of 50, and standard Gibbs energy of reactions, $-\Delta G_r^0 \in [10^3, 10^5]$ J mol^{-1} in steps of 10^3 J mol^{-1}. The colour gradient shows the number of modelled niches: $N = 10$ (red) to $N = 1000$ (green).

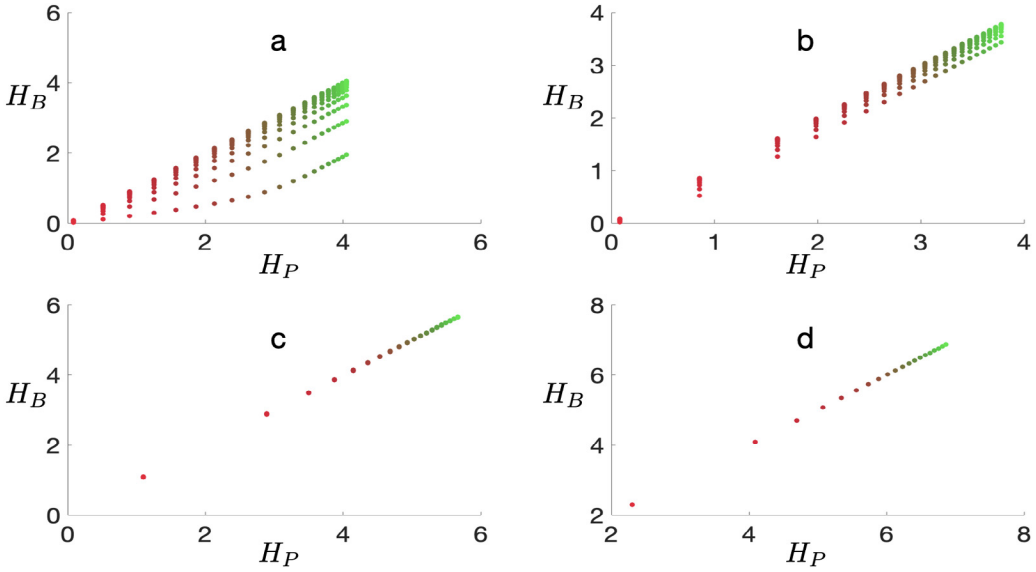

Fig. 4. H_B vs. H_P when a distribution of input substrate concentrations of the form $S_{0i} \sim S_0\, e^{-\frac{(i-N/2)^2}{\sigma^2 N^2}}$ is considered (see SI for details). The remaining model parameters are common to all niches. Each graphic shows all pairs (H_P, H_B) corresponding to the considered instances of $N \in [10, 1000]$, and $-\Delta G_r^0 \in [10^3, 10^5]$ J mol^{-1}. In each case, the departure from a well defined curve indicates that H_P fails to uniquely determine H_B. The graphics correspond to: **a** $\sigma = 0.001$; **b** $\sigma = 0.01$; **c** $\sigma = 0.1$; **d** $\sigma = 1$. The colour gradient is as in Fig. 3.

even though it is the most energetically advantaged (i.e it has the highest S_{0i} and ΔG_r^{0i} values). This asymmetric behaviour across energy scales clearly emerges from the combined effect of all the above model scenarios. At a high energy scale, the percentage difference between the most energetically advantaged niches and those with baseline values for E_{eq}^i, is relatively small and of little relevance. Therefore the effect of the efficiency-cost trade-off becomes more significant. This explains why, for high energy scales, the most viable niches correspond to those with moderate values for both r_{max}^i and P_{0i} (Fig. 11).

4. Variability of H_P and H_B across a chemical gradient

The Gibbs energy of a reaction is dependent on the activities (the product of activity coefficient and concentration) of reactants and products. Hence, even if the concentrations of reactants and products are kept constant, the Gibbs energy of a reaction might change due to changes in activity coefficients, which are dependent on environmental factors such as salinity. We consider here the ideal case where the concentration of one compound, acting as a substrate or product in all oxidation reactions of S_i, is fixed at different values across a series of independent systems. The activity coefficient of this compound is kept constant so that only variability in concentration causes variability in activity. As an example, we take such a compound to be H^+. We assume the fluxes of limiting substrates to be the same for all systems. Hence, we investigate how survival diversity varies along a pH gradient. In particular, if the cells in the ith niche act as H^+-producers, the chemical reaction involving the ith substrate is of the form

$$S_i + reactants \longrightarrow n_i H^+ + products$$

Following the same reasoning that led to Eq. (3), we find

$$\hat{E}_i(s_i) = -\Delta G_r^{0i} + RT \ln s_i - n_i RT \ln[H^+], \tag{18}$$

and taking into account that $pH = -\log_{10}[H^+]$, the available energy in the ith niche (H^+-producers) depends on pH as

$$\hat{E}_i(s_i) = -\Delta G_r^{0i} + RT \ln s_i + n_i RT\, pH \ln 10.$$

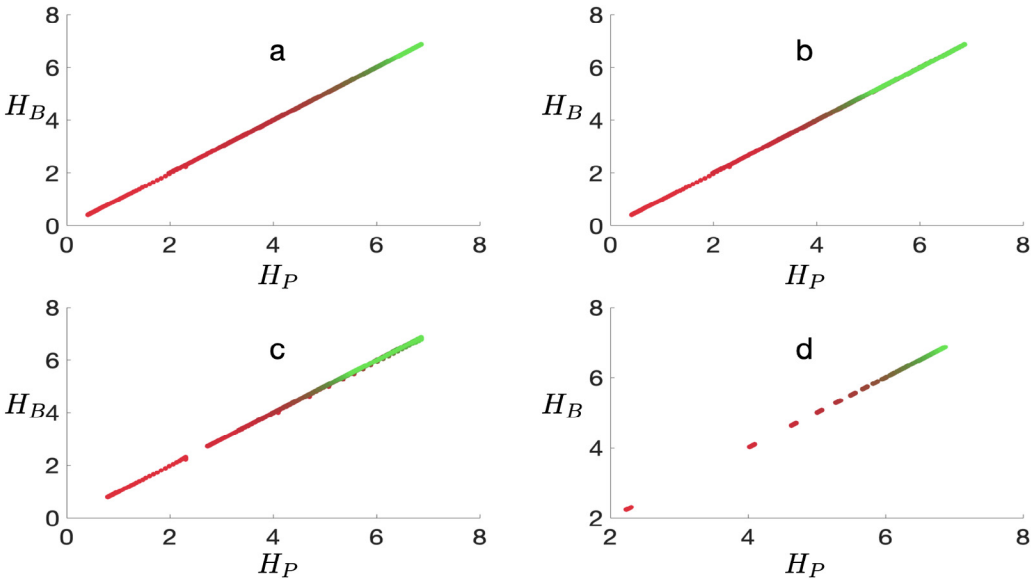

Fig. 5. H_B vs. H_P when a distribution of reaction Gibbs energies of the form $\Delta G_r^{0i} \sim \Delta G_r^0 \, e^{-\frac{(i-N/2)^2}{\sigma^2 N^2}}$ is considered (see SI for details). The remaining model parameters are common to all niches. Each graphic shows all pairs (H_P, H_B) corresponding to the considered instances of $N \in [10, 1000]$, and $-\Delta G_r^0 \in [10^3, 10^5]$ J mol^{-1}. The graphics correspond to: **a** $\sigma = 0.001$; **b** $\sigma = 0.01$; **c** $\sigma = 0.1$; **d** $\sigma = 1$. The colour gradient is as in Fig. 3.

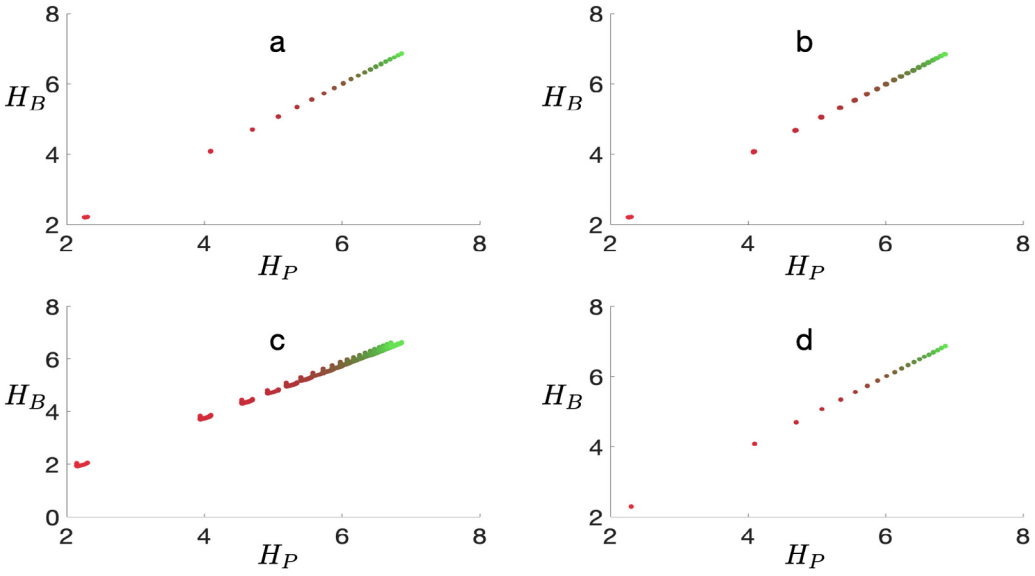

Fig. 6. H_B vs. H_P when a trade-off between uptake rates and maintenance powers of the form $r_{max}^i \sim r_{max} e^{-\frac{(i-N/2)^2}{\sigma^2 N^2}}$ and $P_{0i} \sim P_0 e^{-\frac{(i-N/2)^2}{\sigma^2 N^2}}$, respectively, is considered (see SI for details). The remaining model parameters are common to all niches. Each graphic shows all pairs (H_P, H_B) corresponding to the considered instances of $N \in [10, 1000]$, and $-\Delta G_r^0 \in [10^3, 10^5]$ J mol^{-1}. The graphics correspond to: **a** $\sigma = 0.001$; **b** $\sigma = 0.01$; **c** $\sigma = 0.1$; **d** $\sigma = 1$. The colour gradient is as in Fig. 3.

In the general case,

$$\hat{E}_i(s_i) = -\Delta G_r^{0i} + RT \ln s_i + \kappa_i n_i RT \, pH \, \ln 10\,, \tag{19}$$

where n_i is the proton stoichiometry coefficient for the reaction of the ith substrate and κ_i is either $+1$, if H^+ is a product, or -1 if it is a reactant. The stationary solutions thus depend explicitly on the pH, which entails the pH-dependence of both the survival and power supply diversities (see SI for details)

$$H_B(pH) = -\sum_i \hat{b}_i(pH) \ln\left(\hat{b}_i(pH)\right)\,, \tag{20a}$$

$$H_P(pH) = -\sum_i \hat{P}_s^i(pH) \ln\left(\hat{P}_s^i(pH)\right)\,, \tag{20b}$$

with $\hat{b}_i(pH) = \frac{c_i^*(pH)}{\sum_j c_j^*(pH)}$ and $\hat{P}_s^i(pH) = \frac{S_{0i}\hat{E}_{eq}^i(pH)}{\sum_j S_{0j}\hat{E}_{eq}^j(pH)}$. How the survival diversity changes with pH is, within our modelling framework, largely dependent on the exact chemical and biological setting of the system. In a system where the only relevant difference among the organisms is that H^+ is produced by a fraction of them and consumed by the rest, a decrease in pH (i.e. increase in H^+) causes an increase of the power supply to the consumer of H^+ whereas it makes the power supply to the producers decrease. This is easily checked using Eq. (19), from which we readily see that $\frac{\partial E_i}{\partial pH} < 0$ for the H^+-consumers while $\frac{\partial E_i}{\partial pH} > 0$ for the producers. In this scenario, the available energies at population equilibrium (E_{eq}^i) for H^+-consumers and producers may diverge from each other (Fig. 14c) or converge to each other and cross (Fig. 15c). This reflects in the corresponding stationary cellular abundances in the niches (Figs. 14a and 15a). The effect on the survival diversity is either a monotonic decrease (Fig. 14b) or the presence of a global maximum (Fig. 15b). However, under more complex biological settings, H_B may depend on pH in a highly non-trivial way. As an

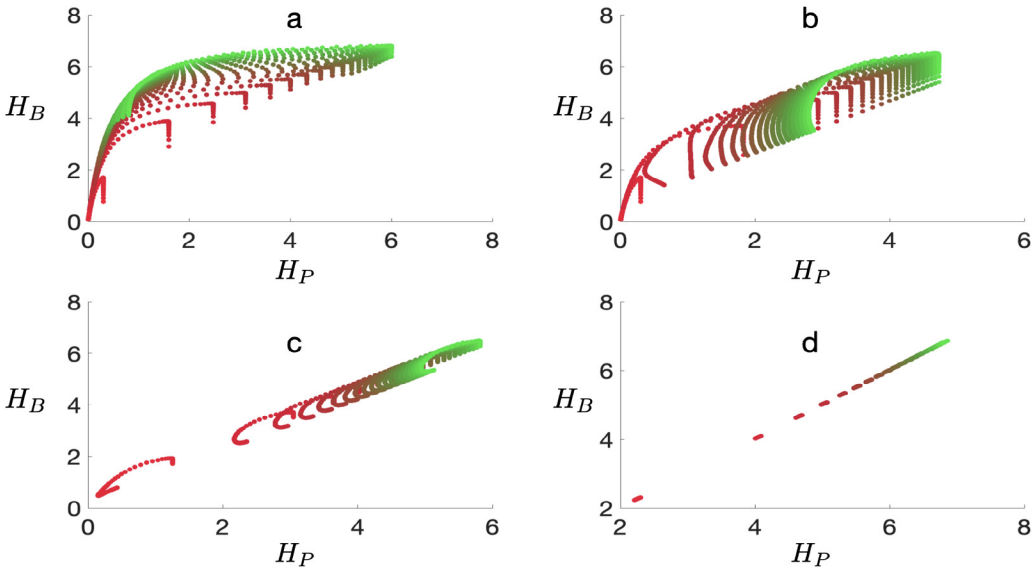

Fig. 7. H_B vs. H_P when unimodal distributions of S_{0i}, $-\Delta G_r^{0i}$, r_{max}^i and P_{0i} are considered simultaneously (see SI for details). Each graphic shows all pairs (H_P, H_B) corresponding to the considered instances of $N \in [10, 1000]$, and $-\Delta G_r^0 \in [10^3, 10^5]$ J mol^{-1}. The graphics correspond to: **a** $\sigma = 0.001$; **b** $\sigma = 0.01$; **c** $\sigma = 0.1$; **d** $\sigma = 1$. The colour gradient is as in Fig. 3.

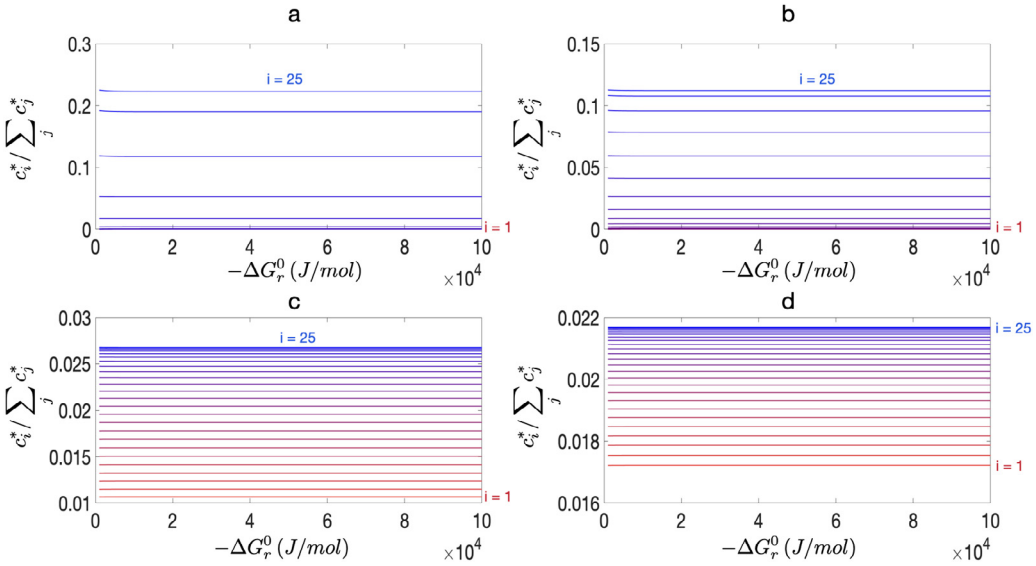

Fig. 8. Survival probability across niches as a function of the reaction standard Gibbs energy ΔG_r^0 when a non-uniform distribution of the input substrate concentrations $S_{0i} \sim S_0\, e^{-\frac{(i-N/2)^2}{\sigma^2 N^2}}$, is considered while the remaining parameters are set as common to all niches (see SI for details). The number of modelled niches N is set to 50 and due to the symmetry of the distribution, only the niches labelled 1–25 are shown. The colour gradient indicates the niche label (red corresponds to $i = 1$ and blue to $i = 25$). The graphics correspond to: **a** $\sigma = 0.05$; **b** $\sigma = 0.1$; **c** $\sigma = 0.5$; **d** $\sigma = 1$.

example of this, here we consider the case of a trade-off between uptake rates and maintenance power given by $r_{max}^i \sim r_{max} e^{-\frac{(i-N/2)^2}{0.01N^2}}$ and $P_{0i} \sim P_m e^{-\frac{(i-N/2)^2}{0.01N^2}}$, respectively, with N denoting the number of modelled niches (Fig. 16). Interestingly, while the dependence of H_P on pH is essentially the same as in the case where all niches share all the relevant parameters (Figs. 15d and 16d), the survival diversity shows a very complex dependence on pH with multiple local maxima and minima (Fig. 16b). In general, pH shapes the relationships between H_B and H_P in rather complex and non-intuitive ways, even within a very simple model such as ours (Figs. 17 and 18). We remark that the ways pH modifies these relationships, depend strongly on the particular values of ΔG_r^{0i} for the chemical reactions used in the microbial niches and the specific proton stoichiometry coefficients.

These analyses demonstrate how H_B can vary along a pH gradient, due to a thermodynamic dependency between pH and power supply. Within our modelling framework, the connections between pH and survival diversity will be similar between systems hosting the same biological niches, but can be very different between systems hosting different biological niches.

5. Discussion

This study provides a comprehensive theoretical analysis of the coupling between fluxes of chemical energy and microbial survival without interspecific competition for resources. We consider a highly idealized population dynamics model where growth is energy limited, which arguably is the case for most of microbial Earth's biosphere [53]. Our model is derived from a few fundamental principles relating chemical

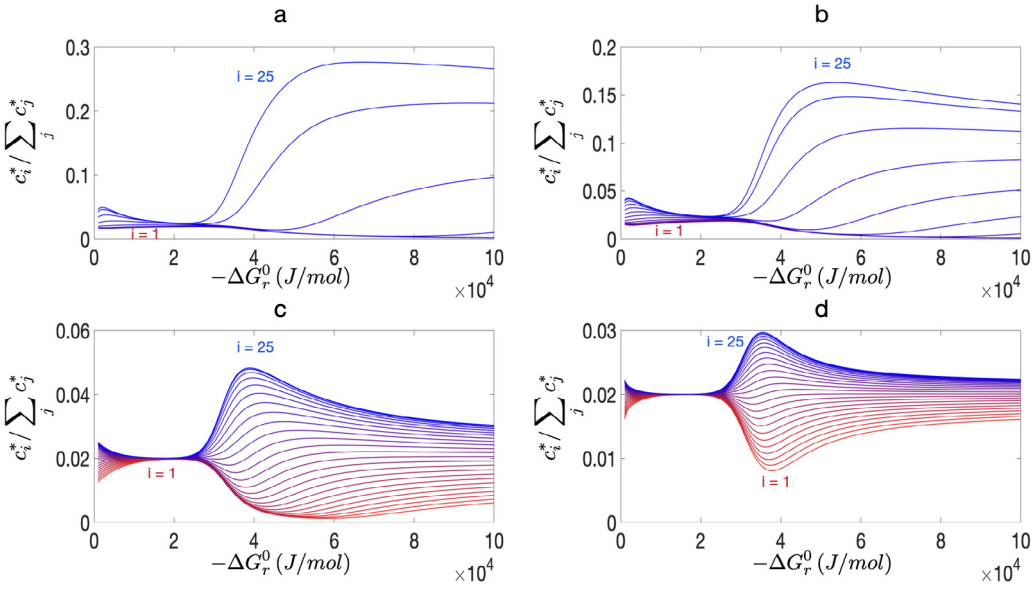

Fig. 9. Survival probability across niches as a function of ΔG_r^0 when a non-uniform distribution of the standard Gibbs energy of reactions of the form $\Delta G_r^{0i} \sim \Delta G_r^0 e^{-\frac{(i-N/2)^2}{\sigma^2 N^2}}$, is considered while the remaining parameters are set as common to all niches (see SI for details). N = 50 and the colour code is the same as in Fig. 8. The graphics correspond to: **a** $\sigma = 0.05$; **b** $\sigma = 0.1$; **c** $\sigma = 0.5$; **d** $\sigma = 1$.

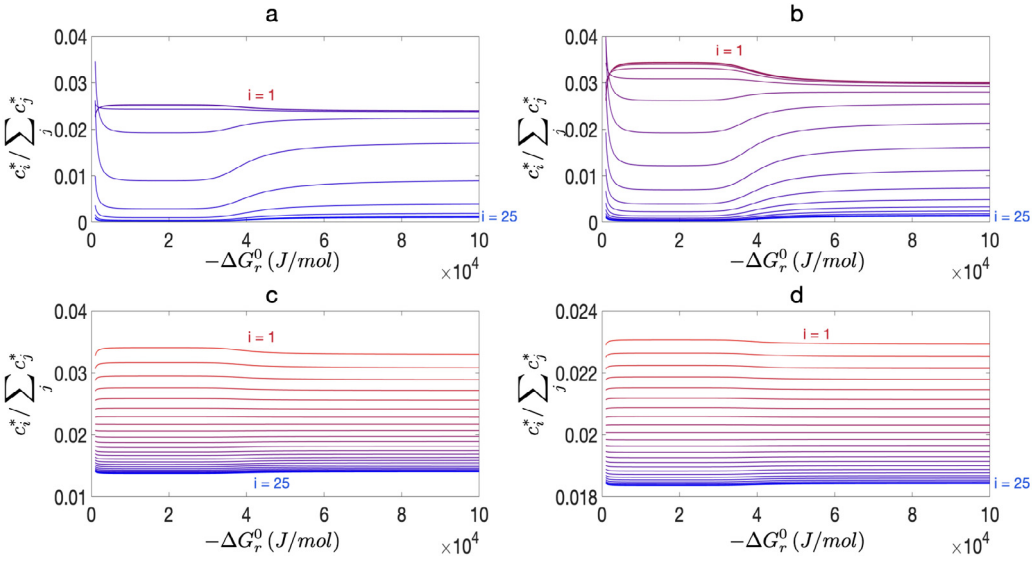

Fig. 10. Survival probability across niches as a function of ΔG_r^0 when a trade-off between uptake rates and maintenance powers of the form $r^i_{max} \sim r_{max} e^{-\frac{(i-N/2)^2}{\sigma^2 N^2}}$ and $P_{0i} \sim P_0 e^{-\frac{(i-N/2)^2}{\sigma^2 N^2}}$, respectively, is considered. The remaining parameters are set as common to all niches (see SI for details). N = 50 and the colour code is the same as in Fig. 8. The graphics correspond to: **a** $\sigma = 0.05$; **b** $\sigma = 0.1$; **c** $\sigma = 0.5$; **d** $\sigma = 1$.

power supply to a system, cellular rates of substrate uptake, cellular power demands, and population size. Our model describes a one species-one resource scenario under a multiplicity of environmental conditions, and investigates how the different bio-chemical factors affect the survival probability. We find that fluxes of energy influence the survival patterns in non-intuitive ways.

The model parameters have a clear relevance to real ecosystems. For example, λ may describe the flow rate of substrates into and out of a fermentor or river discharge into and out of a lake; values of S_{0i} describe concentrations of substrate in the inflow; ΔG_r^0 levels describe typical reaction standard Gibbs energy corresponding to substrate oxidation under given environmental conditions, and ΔG_r^{0i} values describe substrate-specific standard Gibbs energy. This study demonstrates that even within a simple and highly idealized model framework, complex relationships emerge between the energetic setting of a system and microbial survival where distributions of S_{0i} and ΔG_r^{0i}, as well as ΔG_r^0 levels, contribute to shaping niches in distinct ways. Adding a biological trade-off between energy acquisition efficiency and maintenance power increases this complexity even further.

Our numerical experiments demonstrate that a global scaling of ΔG_r^0 is sufficient to create changes in survival patterns. Interestingly, ΔG_r^0 levels also seem to have a large impact on the identity of the most viable niche in models where both ΔG_r^{0i} and S_{0i} values vary and a trade-off between P_{0i} and r^i_{max} is considered (Fig. 11). Although values of ΔG_r^{0i} will rarely change with a common factor for all energy yielding reactions along a chemical gradient, the energy scale ΔG_r^0 is a potentially important parameter for understanding how environmental conditions shape the overall distribution of microbial niches. Changing the power supply to a system by a scaling of λ has a fundamentally different effect on H_B than if the same increase in power supply occurs due to a global scaling of S_{0i} values – i.e. within our modelling framework, H_B remains unaffected by a scaling of λ but responds to a scaling of S_{0i}

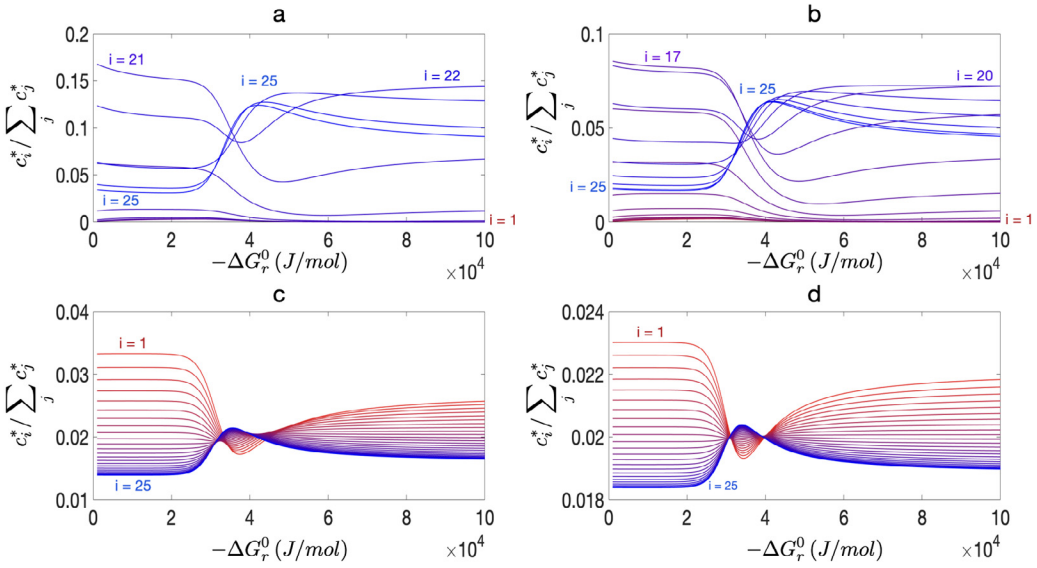

Fig. 11. Survival probability across niches as a function of ΔG_r^0 for distributions $S_{0i} \sim S_0\, e^{-\frac{(i-N/2)^2}{\sigma^2 N^2}}$, $\Delta G_r^{0i} \sim \Delta G_r^0\, e^{-\frac{(i-N/2)^2}{5\sigma^2 N^2}}$, $r_{max}^i \sim r_{max} e^{-\frac{(i-N/2)^2}{\sigma^2 N^2/2}}$ and $P_{0i} \sim P_0 e^{-\frac{(i-N/2)^2}{\sigma^2 N^2/2}}$ (see SI for details). The number of niches is set to $N = 50$. The colour code is the same as in Fig. 8. The graphics correspond to: **a** $\sigma = 0.05$; **b** $\sigma = 0.1$; **c** $\sigma = 0.5$; **d** $\sigma = 1$.

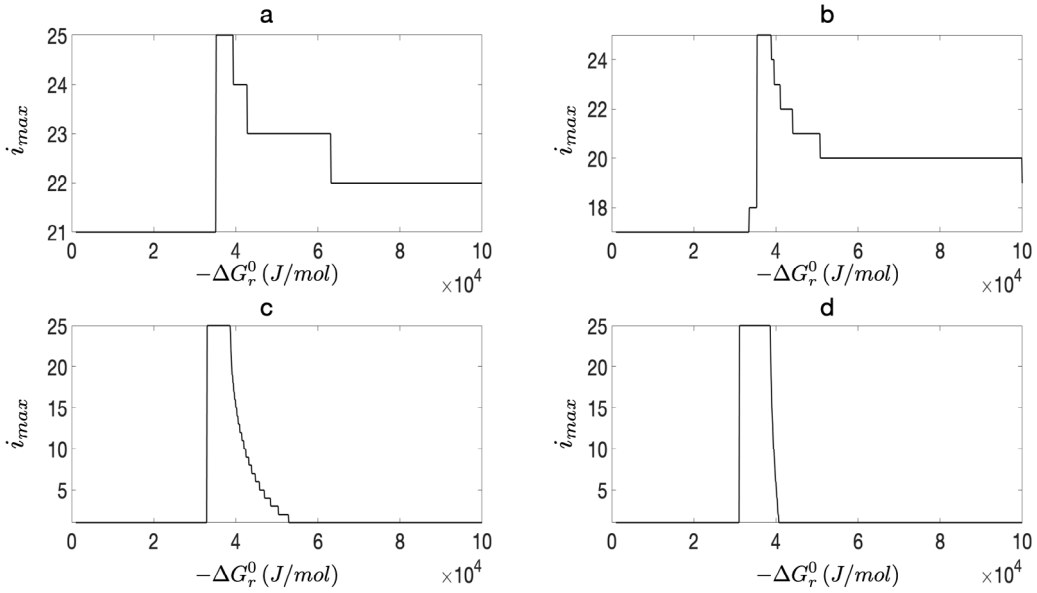

Fig. 12. Label of the most viable niche as a function of ΔG_r^0. The graphics show the most viable niche (dented as i_{max}) corresponding to: **a** Fig. 11a; **b** Fig. 11b; **c** Fig. 11c; **d** Fig. 11d.

values, particularly for low $-\Delta G_r^0$ values (Fig. S2). This result has a clear relevance to natural systems. For example, if we want to predict the niche structure in an ecosystem, then the concentration of substrates in fluids flowing into the system may be a stronger predictor than the rate of fluid inflow. Note that variability in S_{0i} does not affect the chemical composition of the system (except for niche viability). Consequently, environments with identical *in situ* environmental conditions may still host niche structures with different H_B due to differences in the mode of power supply.

Despite the emergent complexity of the connections between energy supply and survival diversity, our results suggest that the diversity of power supply (H_P) may be an overall good predictor for survival diversity (H_B), at least across environments with unimodal distributions for S_{0i}, ΔG_r^{0i}, r_{max}^i and P_{0i} (Figs. 3–7). We stress, however, that a strong correlation between H_P and H_B does not imply that chemical gradients shape niche patterns in a simple way. Rather, as exemplified by our analysis of survival diversity along a pH gradient, variations in the activity of a single chemical compound may have very different effects on the relationship between H_P and H_B under different chemical and biological settings (Figs. 17 and 18). Heterogeneity in the relationship between pH and microbial community structure has been observed in different environments. In a study of 431 geographically widespread and environmentally disparate lakes, no correlation was found between α–diversity and pH [54]. In contrast, pH has been found to be a major driver of soil communities and is often reported to be one of the strongest predictors of α-diversity [1,55]. Reported trends in the relationship between pH and microbial α-diversity in soil also differ. In an analysis of 300 grassland and forest soils in Germany, α-diversity increased with pH from pH 3 to pH 7.5, but with a plateau around pH 5 – 6 [1]. In analyses of numerous types of US soil samples, covering a pH range of 3–9, the α-diversity peaked at pH around 6–7. The diversity patterns observed in soils globally seem to emerge from an aggregation of multiple simpler relationships between pH and the relative abundance of individual taxonomic groups from phylum

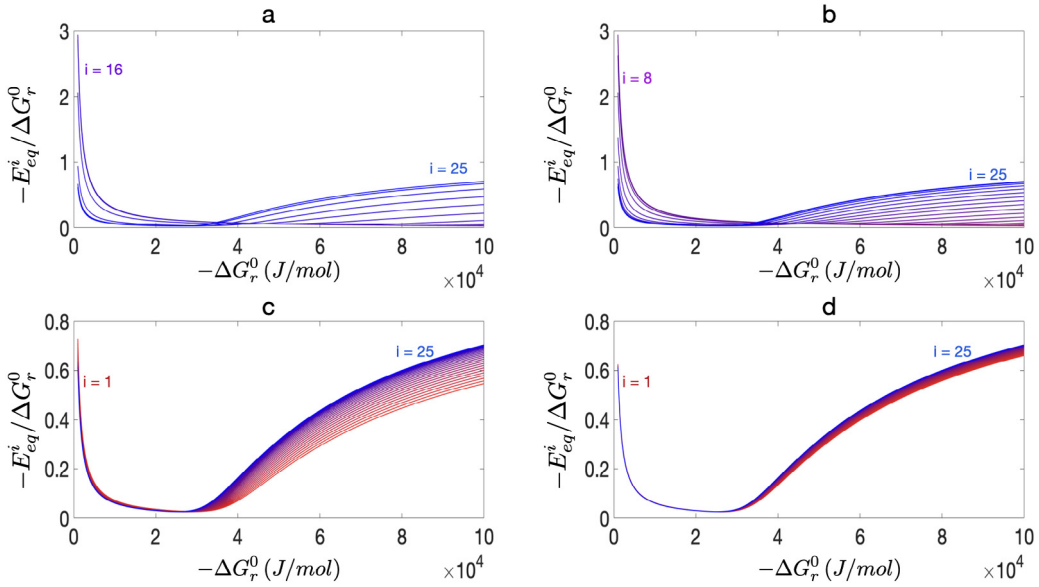

Fig. 13. Available energy, E^i_{eq}, as a function of ΔG^0_r corresponding to the survival probability shown in Fig. 11. The graphics show the available energy corresponding to the survival probability in: **a** Fig. 11a; **b** Fig. 11b; **c** Fig. 11c; **d** Fig. 11d.

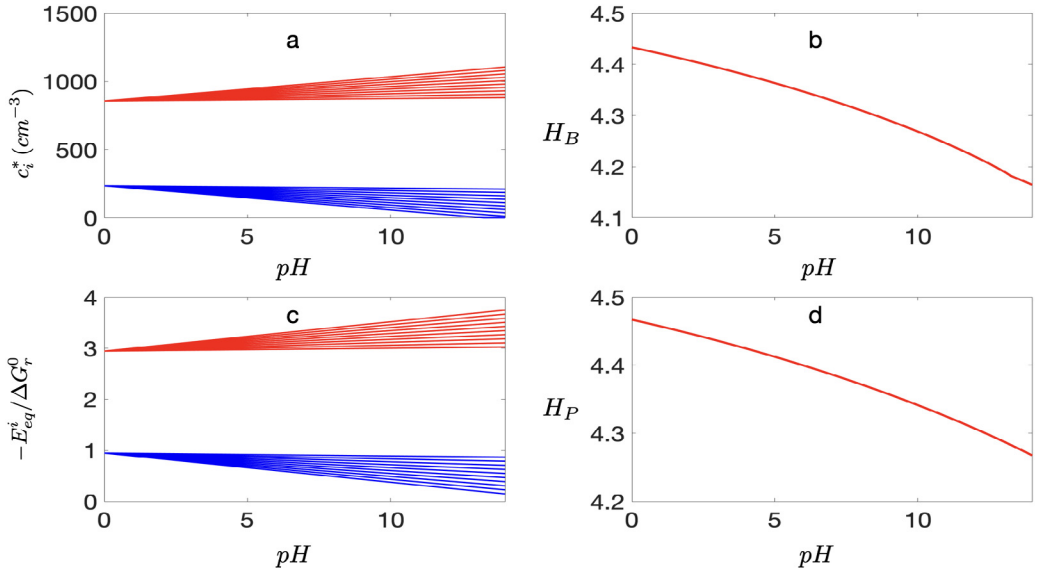

Fig. 14. Effect of pH on H_B and H_P. The model parameters are common to all niches and given the values in Fig. 1b. The number of modelled niches is set to $N = 100$. Half of them are set to be H^+-producers and the other half are H^+-consumers. The H^+-stoichiometric coefficients are assigned values between 1 and 10. The reaction standard Gibbs energy is set to $-\Delta G^0_r = 10^6$ J mol^{-1} for the H^+-consumers and $-\Delta G^0_r = 3 \times 10^6$ J mol^{-1} for the H^+-producers. The graphic **a** shows the abundance of cells for the H^+-consumers (blue line) and for the H^+-producer (red line); The graphic **b** shows the corresponding survival diversity; Graphic **c** shows the pH-dependence of E^i_{eq} corresponding to the plot **a**. The red line shows E_{eq} for the H^+-producer and the blue line corresponds to the H^+-consumer; The plot **d** shows the corresponding power supply diversity (H_P).

to species level [1,56–58]. Intriguingly, this emergence of complexity from simple pH dependence of cellular abundances is what we find in our model (Figs. 15–16).

Whether this type of interdependences are also found between power supply and community structure when interspecific competition for resources is considered, is clearly a topic for future research. Our findings set a promising precedent for these investigations. We remark again that simple environments as the one considered in our work can be reconstructed using microbial strains from culture collections, as artificial communities in laboratory settings and hence our modelling results are potentially testable. Based on our results, we propose three expectations that can act as working hypotheses for further enquiry:

- ΔG^0_r levels and the shape of the distributions of S_{0i} and ΔG^{0i}_r influence microbial biodiversity in different ways. Relative abundance of species (also H_B) is more sensitive to variations in the ΔG^{0i}_r distribution than to comparable variation in the distribution of S_{0i} values.
- H_P is a useful predictor for H_B across environments with similar ΔG^0_r levels and similarly shaped distributions of S_{0i} and ΔG^{0i}_r.
- There is no general trend between a given chemical gradient and biodiversity, rather the relationship between them depends on the thermodynamic setting of the environment.

These expectations can be tested directly under chemostat conditions where chemical fluxes and the chemical composition of the system can be controlled, and microbial communities can be easily monitored – e.g. through 16S rRNA gene sequence analyses. In order to set up an experimental system comparable to what is modelled here, the species

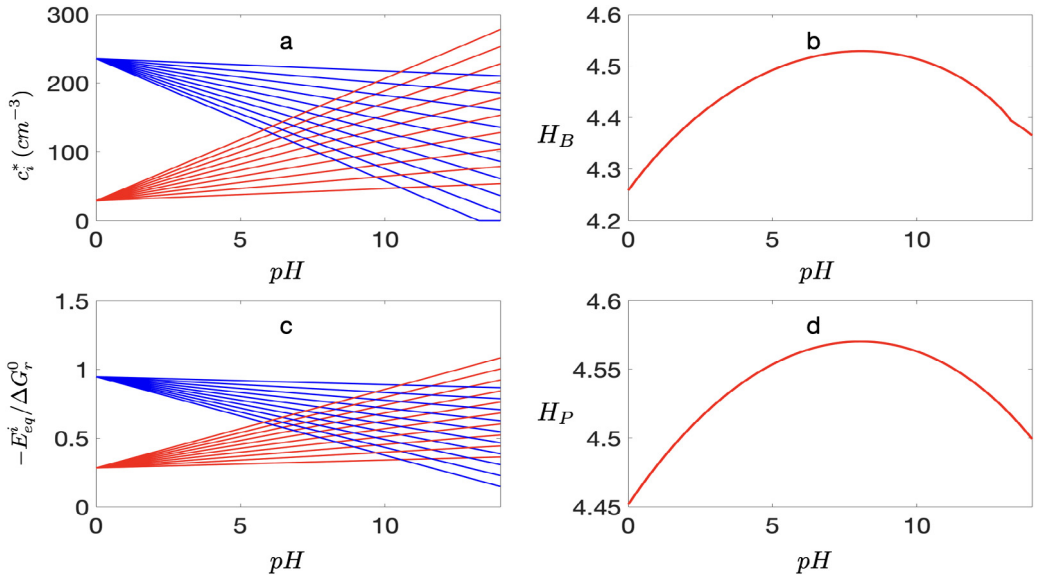

Fig. 15. Effect of pH on H_B and H_P. The ΔG_r^0 for the H^+-consumers is set to -10^6 J mol^{-1} while for the H^+-producers, $\Delta G_r^0 = -3 \times 10^5$ J mol^{-1}. The colour code and the remaining model parameters are as in Fig. 14.

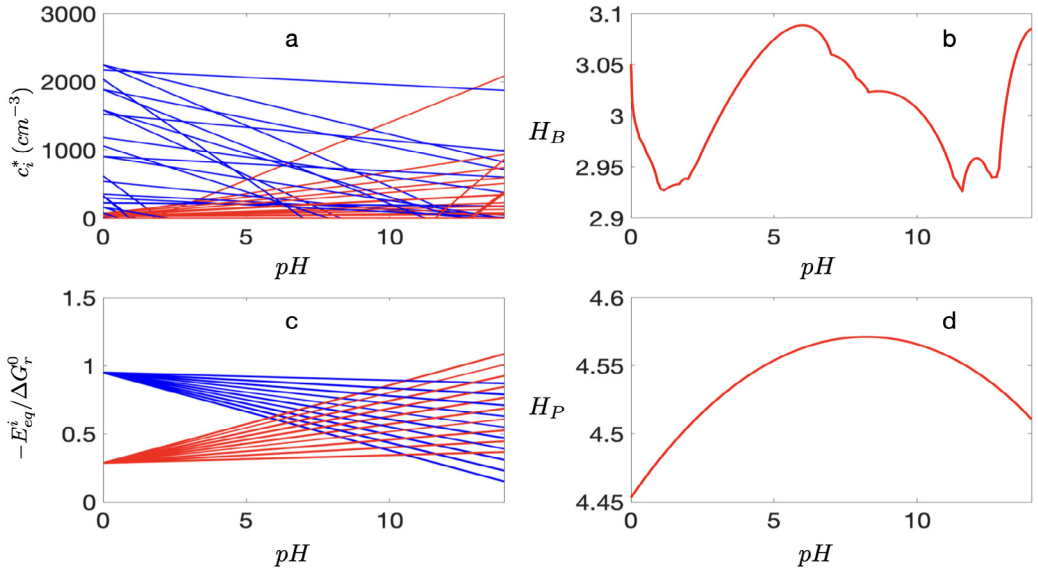

Fig. 16. Effect of pH on H_B and H_P, considering a trade-off between uptake rates and maintenance powers given by: $r_{max}^i = r_{max}\left(e^{-\frac{(i-N/2)^2}{0.01N^2}} + \frac{1}{100}\right)$ and $P_{0i} = P_0\left(e^{-\frac{(i-N/2)^2}{0.01N^2}} + \frac{1}{20}\right)$, with $N = 100$. The ΔG_r^0 for the H^+-consumers is set to -10^6 J mol^{-1} while for the H^+-producers, $\Delta G_r^0 = -3 \times 10^5$ J mol^{-1}. The colour code and the remaining model parameters are as in Fig. 14.

grown in the chemostat should have distinct substrate spectra so that each species acquires energy by the oxidation of one limiting substrate each. In principle, one could analyse diversity patterns in a system with only two species, but a higher number of species may be desirable for a more robust analysis. Estimates of maintenance power can be obtained experimentally, taking into account that maintenance power depends on environmental conditions, such as temperature [53,59,60].

In the field of microbial ecology, connections between environmental setting and biodiversity in natural systems have thus far mostly been explored through linear regression analyses or multivariate analyses involving directly measurable environmental parameters. Our results suggest that in order to identify driving mechanisms of biodiversity and community structure, a concerted effort should be put into assessing the role of power supply. Quantifying chemical power supply in natural environments can be challenging as it requires accurate information on chemical composition and dominant chemical fluxes in the system. Another complicating factor is that variations in the concentration of a chemical compound may have both direct and indirect effects on energy fluxes. For example, pH influences energy availability directly in energy yielding reactions where protons act as reactants or products, but also indirectly by modulating the activity coefficient or chemical speciation of numerous chemical compounds [26]. Hence, there is a need to develop improved methods for estimating energy fluxes and including such estimates in ecological studies to test model predictions.

6. Conclusions

In this work, we have performed a thorough mathematical analysis of the relationship between microbial survival and chemical power supply in an energy limited environment and without interspecific competition for resources, by considering a one species-one resource model under multiple environmental and biological conditions. Our study

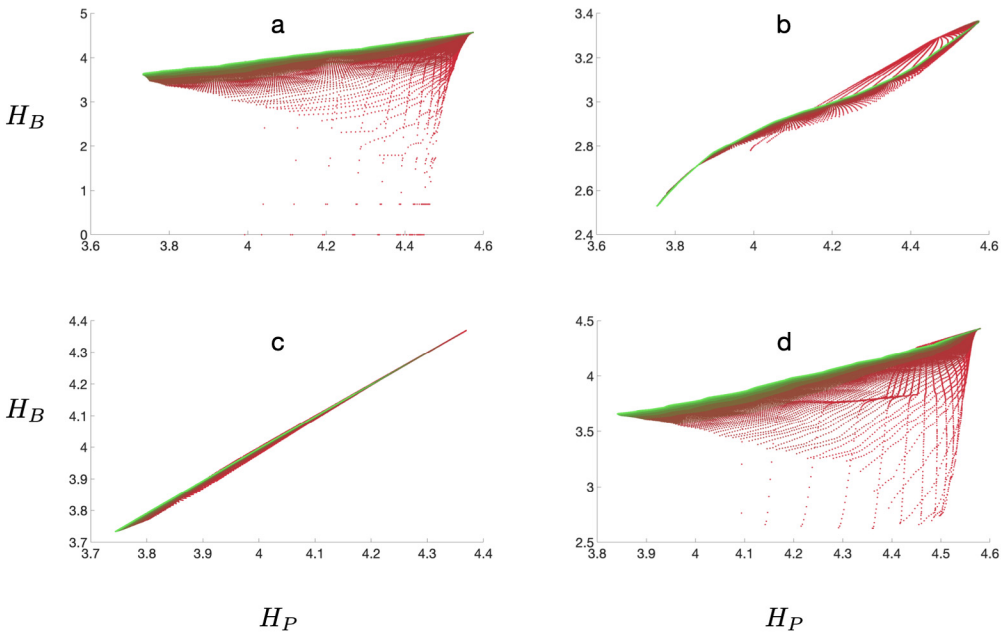

Fig. 17. H_B vs. H_P when the effect of pH is considered. The plots show the pairs (H_P, H_B) corresponding to all the considered instances of $pH \in [0, 14]$ and $-\Delta G_r^0 \in [1, 10] \times 10^5$ J mol^{-1}. $N = 100$ and half of the niches are set as H^+-producers and the other half are H^+-consumers. The proton stoichiometry coefficients are assigned values between 1 and 10 (see SI for details). The colour gradient corresponds to pH = 0 (red) to pH = 14 (green). The graphics correspond to (see SI for details): **a** All niches share the values for the relevant parameters; **b** A distribution $S_{0i} \sim S_0\, e^{-\frac{(i-N/2)^2}{0.01N^2}}$ is considered; **c** A distribution $\Delta G_r^{0i} \sim \Delta G_r^0\, e^{-\frac{(i-N/2)^2}{0.05N^2}}$ is considered; **d** A trade-off between uptake rates and maintenance powers as $r^i_{max} \sim r_{max}\, e^{-\frac{(i-N/2)^2}{0.01N^2/2}}$ and $P_{0i} \sim P_0\, e^{-\frac{(i-N/2)^2}{0.01N^2/2}}$ is considered.

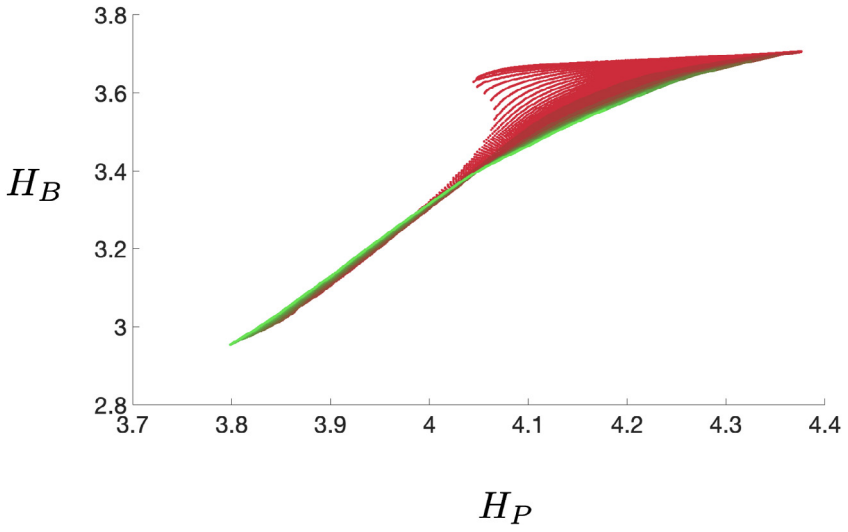

Fig. 18. H_B vs. H_P when the effect of pH is considered and unimodal distributions for the relevant parameters are considered simultaneously (see SI for details). The colour gradient and the ranges for pH and for ΔG_r^0 are as in Fig. 17.

forms a baseline for future theoretical exploration of the coupling between power supply and biological diversity in models of more complex ecosystems accounting for competition and syntrophic associations. We find a strong coupling between the diversity in chemical power supply and microbial survival patterns, while the individual factors determining power supply - i.e. substrate concentrations in fluids entering a system, fluid flowrates, and Gibbs energies of reactions — affect the microbial survival in fundamentally distinct ways. Moreover, we show how complex survival patterns along various chemical gradients can emerge from simple connections between power supply and growth. This study provides a thermodynamics based framework for microbial survival modelling, and highlights the importance of including careful analyses of power supply in ecological studies aiming at deciphering how environmental conditions shape microbial communities. Our findings highlight the importance of taking into account energy supply and energy utilization in microbial systems in order to advance our understanding of how the fundamental laws of thermodynamics shape the biosphere.

Software: The code to reproduce the numerical results presented in this work is available as Jupyter notebooks in github.com/diegocastro79/Power-Supply-vs-Microbial-Survival

CRediT authorship contribution statement

David Diego: Methodology, Conceptualization, Formal analysis, Software, Writing - original draft. **Bjarte Hannisdal:** Conceptualization, Writing - original draft. **Håkon Dahle:** Methodology, Conceptualization, Writing - original draft.

Declaration of competing interest

The authors declare that they have no known competing financial interests or personal relationships that could have appeared to influence the work reported in this paper.

Acknowledgements

This work was supported by the K.G. Jebsen Center for Deep Sea Research and by a Trond Mohn Foundation, Norway Starting Grant to B.H.

Appendix A. Supplementary data

Supplementary material related to this article can be found online at https://doi.org/10.1016/j.mbs.2021.108615.

References

[1] K. Kaiser, B. Wemheuer, V. Korolkow, F. Wemheuer, H. Nacke, I. Schöning, M. Schrumpf, R. Daniel, Driving forces of soil bacterial community structure, diversity, and function in temperate grasslands and forests, Sci. Rep. 6 (1) (2016) 1–12.
[2] S. Zhao, J.-J. Liu, S. Banerjee, N. Zhou, Z.-Y. Zhao, K. Zhang, C.-Y. Tian, Soil pH is equally important as salinity in shaping bacterial communities in saline soils under halophytic vegetation, Sci. Rep. 8 (1) (2018) 1–11.
[3] T. Pommier, B. Canbäck, L. Riemann, K.H. Boström, K. Simu, P. Lundberg, A. Tunlid, Å. Hagström, Global patterns of diversity and community structure in marine bacterioplankton, Mol. Ecol. 16 (4) (2007) 867–880.
[4] J.A. Fuhrman, Microbial community structure and its functional implications, Nature 459 (7244) (2009) 193–199.
[5] J. Yang, H. Jiang, G. Wu, H. Dong, et al., Salinity shapes microbial diversity and community structure in surface sediments of the Qinghai-Tibetan Lakes, Sci. Rep. 6 (2016) 25078.
[6] K. Zhang, Y. Shi, X. Cui, P. Yue, K. Li, X. Liu, B.M. Tripathi, H. Chu, Salinity is a key determinant for soil microbial communities in a desert ecosystem, MSystems 4 (1) (2019).
[7] A. Vidal-Durà, I.T. Burke, R.J. Mortimer, D.I. Stewart, Diversity patterns of benthic bacterial communities along the salinity continuum of the humber estuary (UK), Aquatic Microbial Ecol. 81 (3) (2018) 277–291.
[8] H. Osterholz, D.L. Kirchman, J. Niggemann, T. Dittmar, Diversity of bacterial communities and dissolved organic matter in a temperate estuary, FEMS Microbiol. Ecol. 94 (8) (2018) fiy119.
[9] V. Hubalek, X. Wu, A. Eiler, M. Buck, C. Heim, M. Dopson, S. Bertilsson, D. Ionescu, Connectivity to the surface determines diversity patterns in subsurface aquifers of the Fennoscandian shield, ISME J. 10 (10) (2016) 2447–2458.
[10] C. Magnabosco, L.-H. Lin, H. Dong, M. Bomberg, W. Ghiorse, H. Stan-Lotter, K. Pedersen, T. Kieft, E. Van Heerden, T.C. Onstott, The biomass and biodiversity of the continental subsurface, Nat. Geosci. 11 (10) (2018) 707–717.
[11] R.E. Antwis, S.M. Griffiths, X.A. Harrison, P. Aranega-Bou, A. Arce, A.S. Bettridge, F.L. Brailsford, A. de Menezes, A. Devaynes, K.M. Forbes, et al., Fifty important research questions in microbial ecology, FEMS Microbiol. Ecol. 93 (5) (2017) fix044.
[12] T. Großkopf, O.S. Soyer, Synthetic microbial communities, Curr. Opin. Microbiol. 18 (2014) 72–77.
[13] T. Großkopf, O.S. Soyer, Microbial diversity arising from thermodynamic constraints, ISME J. 10 (11) (2016) 2725–2733.
[14] I. Gudelj, J.S. Weitz, T. Ferenci, M. Claire Horner-Devine, C.J. Marx, J.R. Meyer, S.E. Forde, An integrative approach to understanding microbial diversity: from intracellular mechanisms to community structure, Ecol. Lett. 13 (9) (2010) 1073–1084.
[15] S. O'Brien, D.J. Hodgson, A. Buckling, The interplay between microevolution and community structure in microbial populations, Curr. Opin. Biotechnol. 24 (4) (2013) 821–825.
[16] S.-B. Hsu, S. Hubbell, P. Waltman, A mathematical theory for single-nutrient competition in continuous cultures of micro-organisms, SIAM J. Appl. Math. 32 (2) (1977) 366–383.
[17] S. Hsu, Limiting behavior for competing species, SIAM J. Appl. Math. 34 (4) (1978) 760–763.
[18] G. Butler, G. Wolkowicz, A mathematical model of the chemostat with a general class of functions describing nutrient uptake, SIAM J. Appl. Math. 45 (1) (1985) 138–151.
[19] G.S. Wolkowicz, Z. Lu, Global dynamics of a mathematical model of competition in the chemostat: general response functions and differential death rates, SIAM J. Appl. Math. 52 (1) (1992) 222–233.
[20] C. Winter, T. Bouvier, M.G. Weinbauer, T.F. Thingstad, Trade-offs between competition and defense specialists among unicellular planktonic organisms: the "killing the winner" hypothesis revisited, Microbiol. Mol. Biol. Rev. 74 (1) (2010) 42–57.
[21] T.F. Thingstad, Elements of a theory for the mechanisms controlling abundance, diversity, and biogeochemical role of lytic bacterial viruses in aquatic systems, Limnol. Oceanogr. 45 (6) (2000) 1320–1328.
[22] S. Louca, A.K. Hawley, S. Katsev, M. Torres-Beltran, M.P. Bhatia, S. Kheirandish, C.C. Michiels, D. Capelle, G. Lavik, M. Doebeli, et al., Integrating biogeochemistry with multiomic sequence information in a model oxygen minimum zone, Proc. Natl. Acad. Sci. 113 (40) (2016) E5925–E5933.
[23] D.C. Reed, C.K. Algar, J.A. Huber, G.J. Dick, Gene-centric approach to integrating environmental genomics and biogeochemical models, Proc. Natl. Acad. Sci. 111 (5) (2014) 1879–1884.
[24] H. Dahle, I. Økland, I.H. Thorseth, R.B. Pederesen, I.H. Steen, Energy landscapes shape microbial communities in hydrothermal systems on the Arctic Mid-Ocean Ridge, ISME J. 9 (7) (2015) 1593–1606.
[25] H. Dahle, S. Le Moine Bauer, T. Baumberger, R. Stokke, R.B. Pedersen, I.H. Thorseth, I.H. Steen, Energy landscapes in hydrothermal chimneys shape distributions of primary producers, Front. Microbiol. 9 (2018) 1570.
[26] Q. Jin, M.F. Kirk, PH as a primary control in environmental microbiology: 1. thermodynamic perspective, Front. Environ. Sci. 6 (2018) 21.
[27] D.E. LaRowe, J.P. Amend, Catabolic rates, population sizes and doubling/replacement times of microorganisms in natural settings, Amer. J. Sci. 315 (3) (2015) 167–203.
[28] R. Marsland III, W. Cui, J. Goldford, A. Sanchez, K. Korolev, P. Mehta, Available energy fluxes drive a transition in the diversity, stability, and functional structure of microbial communities, PLoS Comput. Biol. 15 (2) (2019) e1006793.
[29] A. Goyal, S. Maslov, Diversity, stability, and reproducibility in stochastically assembled microbial ecosystems, Phys. Rev. Lett. 120 (15) (2018) 158102.
[30] J.E. Goldford, N. Lu, D. Bajić, S. Estrela, M. Tikhonov, A. Sanchez-Gorostiaga, D. Segrè, P. Mehta, A. Sanchez, Emergent simplicity in microbial community assembly, Science 361 (6401) (2018) 469–474.
[31] A.R. Zomorrodi, D. Segrè, Synthetic ecology of microbes: mathematical models and applications, J. Mol. Biol. 428 (5) (2016) 837–861.
[32] W.R. Harcombe, W.J. Riehl, I. Dukovski, B.R. Granger, A. Betts, A.H. Lang, G. Bonilla, A. Kar, N. Leiby, P. Mehta, et al., Metabolic resource allocation in individual microbes determines ecosystem interactions and spatial dynamics, Cell Rep. 7 (4) (2014) 1104–1115.
[33] J. Friedman, L.M. Higgins, J. Gore, Community structure follows simple assembly rules in microbial microcosms, Nat. Ecol. Evol. 1 (5) (2017) 1–7.
[34] A. Fernández, S. Huang, S. Seston, J. Xing, R. Hickey, C. Criddle, J. Tiedje, How stable is stable? Function versus community composition, Appl. Environ. Microbiol. 65 (8) (1999) 3697–3704.
[35] A.S. Fernandez, S.A. Hashsham, S.L. Dollhopf, L. Raskin, O. Glagoleva, F.B. Dazzo, R.F. Hickey, C.S. Criddle, J.M. Tiedje, Flexible community structure correlates with stable community function in methanogenic bioreactor communities perturbed by glucose, Appl. Environ. Microbiol. 66 (9) (2000) 4058–4067.
[36] N. Fernandez-Gonzalez, J.A. Huber, J.J. Vallino, Microbial communities are well adapted to disturbances in energy input, MSystems 1 (5) (2016).
[37] L. Wittebolle, M. Marzorati, L. Clement, A. Balloi, D. Daffonchio, K. Heylen, P. De Vos, W. Verstraete, N. Boon, Initial community evenness favours functionality under selective stress, Nature 458 (7238) (2009) 623–626.
[38] X. Wang, X. Wen, H. Yan, K. Ding, F. Zhao, M. Hu, Bacterial community dynamics in a functionally stable pilot-scale wastewater treatment plant, Bioresour. Technol. 102 (3) (2011) 2352–2357.
[39] M. Seto, Y. Iwasa, Population dynamics of chemotrophs in anaerobic conditions where the metabolic energy acquisition per redox reaction is limited, J. Theoret. Biol. 467 (2019) 164–173.
[40] S. Pirt, The maintenance energy of bacteria in growing cultures, Proc. R. Soc. Lond. Ser. B 163 (991) (1965) 224–231.
[41] T.M. Hoehler, B.B. Jørgensen, Microbial life under extreme energy limitation, Nat. Rev. Microbiol. 11 (2) (2013) 83–94.
[42] P. Van Bodegom, Microbial maintenance: a critical review on its quantification, Microb. Ecol. 53 (4) (2007) 513–523.
[43] O. Neijssel, D. Tempest, The role of energy-spilling reactions in the growth of klebsiella aerogenes NCTC 418 in aerobic chemostat culture, Arch. Microbiol. 110 (2–3) (1976) 305–311.
[44] G.M. Cook, J.B. Russell, Energy-spilling reactions of Streptococcus bovis and resistance of its membrane to proton conductance, Appl. Environ. Microbiol. 60 (6) (1994) 1942–1948.
[45] J.B. Russell, H.J. Strobel, ATPase-dependent energy spilling by the ruminal bacterium, streptococcus bovis, Arch. Microbiol. 153 (4) (1990) 378–383.

[46] I.R. Swingland, Biodiversity, definition of, Encyclopedia Biodivers. 1 (2001) 377–391.
[47] M.O. Hill, Diversity and evenness: a unifying notation and its consequences, Ecology 54 (2) (1973) 427–432.
[48] A. Chao, C.-H. Chiu, L. Jost, Unifying species diversity, phylogenetic diversity, functional diversity, and related similarity and differentiation measures through Hill numbers, Annu. Rev. Ecol. Evol. Syst. 45 (2014) 297–324.
[49] R.C. Gatti, N. Amoroso, A. Monaco, Estimating and comparing biodiversity with a single universal metric, Ecol. Model. 424 (2020) 109020.
[50] E. Litchman, K.F. Edwards, C.A. Klausmeier, Microbial resource utilization traits and trade-offs: implications for community structure, functioning, and biogeochemical impacts at present and in the future, Front. Microbiol. 6 (2015) 254.
[51] M.T. Wortel, E. Noor, M. Ferris, F.J. Bruggeman, W. Liebermeister, Metabolic enzyme cost explains variable trade-offs between microbial growth rate and yield, PLoS Comput. Biol. 14 (2) (2018) e1006010.
[52] M. Mori, E. Marinari, A. De Martino, A yield-cost tradeoff governs Escherichia coli's decision between fermentation and respiration in carbon-limited growth, NPJ Syst. Biol. Appl. 5 (1) (2019) 1–9.
[53] T. Hoehler, Biological energy requirements as quantitative boundary conditions for life in the subsurface, Geobiology 2 (4) (2004) 205–215.
[54] J. Yang, H. Jiang, H. Dong, Y. Liu, A comprehensive census of lake microbial diversity on a global scale, Sci. China Life Sci. 62 (10) (2019) 1320–1331.
[55] N. Fierer, R.B. Jackson, The diversity and biogeography of soil bacterial communities, Proc. Natl. Acad. Sci. 103 (3) (2006) 626–631.
[56] H. Nacke, A. Thürmer, A. Wollherr, C. Will, L. Hodac, N. Herold, I. Schöning, M. Schrumpf, R. Daniel, Pyrosequencing-based assessment of bacterial community structure along different management types in German forest and grassland soils, PLoS One 6 (2) (2011) e17000.
[57] C. Will, A. Thürmer, A. Wollherr, H. Nacke, N. Herold, M. Schrumpf, J. Gutknecht, T. Wubet, F. Buscot, R. Daniel, Horizon-specific bacterial community composition of german grassland soils, as revealed by pyrosequencing-based analysis of 16s rRNA genes, Appl. Environ. Microbiol. 76 (20) (2010) 6751–6759.
[58] C.L. Lauber, M. Hamady, R. Knight, N. Fierer, Pyrosequencing-based assessment of soil pH as a predictor of soil bacterial community structure at the continental scale, Appl. Environ. Microbiol. 75 (15) (2009) 5111–5120.
[59] L. Tijhuis, M.C. Van Loosdrecht, J.v. Heijnen, A thermodynamically based correlation for maintenance Gibbs energy requirements in aerobic and anaerobic chemotrophic growth, Biotechnol. Bioeng. 42 (4) (1993) 509–519.
[60] P.B. Price, T. Sowers, Temperature dependence of metabolic rates for microbial growth, maintenance, and survival, Proc. Natl. Acad. Sci. 101 (13) (2004) 4631–4636.